

YbNiB₄: a Kondo lattice with low-dimensional antiferromagnetic fluctuations

This article has been downloaded from IOPscience. Please scroll down to see the full text article.

2009 J. Phys.: Condens. Matter 21 206003

(<http://iopscience.iop.org/0953-8984/21/20/206003>)

View [the table of contents for this issue](#), or go to the [journal homepage](#) for more

Download details:

IP Address: 129.252.86.83

The article was downloaded on 29/05/2010 at 19:45

Please note that [terms and conditions apply](#).

YbNiB₄: a Kondo lattice with low-dimensional antiferromagnetic fluctuations

A Prasad¹, Z Hossain¹, H S Jeevan² and C Geibel²

¹ Department of Physics, Indian Institute of Technology, Kanpur 208016, India

² Max-Planck Institute for Chemical Physics of Solids, 01187 Dresden, Germany

E-mail: zakir@iitk.ac.in

Received 18 November 2008, in final form 12 March 2009

Published 24 April 2009

Online at stacks.iop.org/JPhysCM/21/206003

Abstract

We have grown single crystals of YbNiB₄ using a Ni₆₀B₄₀ flux and determined the magnetic properties of this compound by means of magnetic susceptibility, specific heat and electrical resistivity measurement. Yb ions in YbNiB₄ are in a trivalent state and present a transition from a paramagnetic state to an antiferromagnetic (AF) state at $T_{N1} = 5.4$ K and a further transition towards a second AF state at $T_{N2} = 4.0$ K. Kondo type behavior in the resistivity and an enhanced Sommerfeld coefficient $\gamma = 100$ mJ mol⁻¹ K⁻² provide evidence for a significant Kondo interaction. A broad maximum in $\chi(T)$ at around 8 K, well above T_{N1} , suggests low-dimensional antiferromagnetic correlations. Both mechanisms lead to strong fluctuation in an extended temperature range above T_{N1} , up to the characteristic energy of this system, which was estimated to be $T_{4f} = 16$ K from an analysis of the entropy.

1. Introduction

Yb-based intermetallic compounds are well known for their interesting physical properties. Yb has an unstable f-shell; therefore, by applying external pressure, a magnetic field or by changing composition it can be tuned from the non-magnetic Yb²⁺ (4f¹⁴) state to the magnetic Yb³⁺ (4f¹³) state. At the crossover, one observes unusual properties like, for example, the formation of heavy electrons or of unconventional metallic and/or superconducting states. YbRh₂Si₂ presents a nice example of such behavior, where the magnetic ordered state is suppressed by the application of an external field or doping leading to a quantum critical point (QCP) [1, 2]. The homologous heavy fermion system YbIr₂Si₂ is located on the non-magnetic side of the QCP [3] and therefore shows pressure induced magnetic order [4]. More recently, observation of heavy fermions in the presence of a large orbital degeneracy and of two quantum critical points by application of pressure were reported for a series of YbT₂Zn₂₀ [5] (T = transition metal) compounds and in Yb₂Pd₂Sn [6], respectively. But even systems with a well localized magnetic trivalent Yb state sometimes present unusual features, like quadrupolar ordering in the presence of a quasi-quartet ground state in YbRu₂Ge₂ [7] or magnetic frustration connected with a Shastry–Sutherland

type of magnetic lattice in Yb₂Pt₂Pb [8]. On the other hand, ternary rare earth transition metal borides R–T–B (R = rare earth element) are also well known for the occurrence of interesting phenomena. For example, CeRh₃B₂ [9] presents an exceptionally high ferromagnetic Ce ordering temperature ($T_C \sim 110$ K) and exhibits Kondo lattice behavior. The RRh₄B₄ [10, 11] compound series were among the first examples of interplay between magnetic ordering and superconductivity. These unusual properties are related to specific structural features of B-compounds like two-dimensional B networks, the formation of B–T clusters, or very short interatomic distances, which all result in exceptional electronic properties due to comparatively strong directional hybridization.

Despite this promising context, only a few Yb-based boron compounds have been investigated up to now, because the low boiling point of Yb in connection with the high melting temperature of boron compounds makes sample preparation difficult. Most of the work was devoted to binary Yb–B compounds, where YbB₁₂ [12] is a rare example of a Yb-based Kondo insulator, while YbB₄ [13] was recently suggested to show low-dimensional intermediate valence fluctuations. A further intensively studied Yb–T–B compound is the heavy fermion system YbNi₂B₂C [14, 15]. In order to search

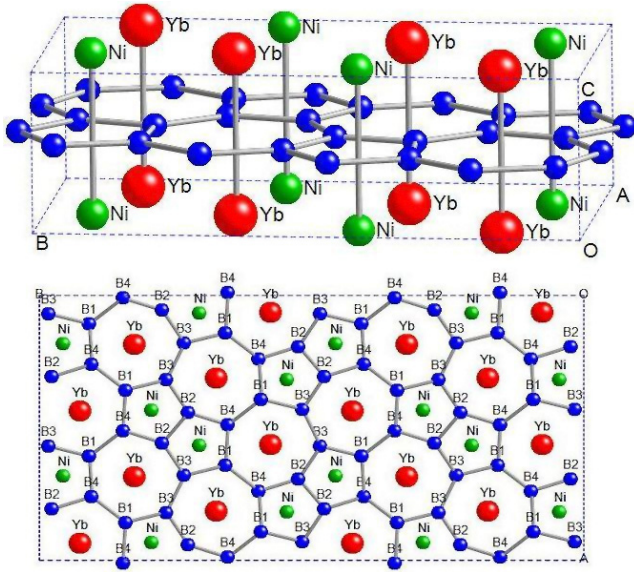


Figure 1. The upper and lower panels present three-dimensional and two-dimensional views of the orthorhombic structure of YbNiB_4 single crystal. Yb (red) and Ni (green) are intercalated between B-layers composed of edge sharing heptagonal and pentagonal boron (blue) rings.

(This figure is in colour only in the electronic version)

for further interesting Yb-based boride we prepared YbNiB_4 single crystals and investigated their physical properties. YbNiB_4 belongs to a large series of isostructural compounds, RTB_4 , crystallizing in the orthorhombic YCrB_4 -type structure. While the structure of these compounds was determined quite a long time ago, the physical properties of the Yb-based compounds have yet not been reported [16, 17]. Very recently, the compound $\beta\text{-YbAlB}_4$, which crystallizes in a very similar structure, attracted much attention because it was proposed to be the first Yb-based heavy fermion system showing unconventional superconductivity at $T_C \approx 80$ mK [18–20]. YbNiB_4 and YbAlB_4 present an interesting two-dimensional structure with Yb and Ni(Al) being intercalated between B-layers composed of edge sharing heptagonal and pentagonal B rings (see figure 1). This structure is similar to that of MgB_2 in which Mg is intercalated between B sheets. MgB_2 shows superconductivity at 39 K and presents a very high critical current value, making this compound quite interesting for industrial applications [21]. This was a further motivation for studying YbNiB_4 .

2. Experimental details

We have grown single crystals of YbNiB_4 using a $\text{Ni}_{60}\text{B}_{40}$ flux. Yb, B and $\text{Ni}_{60}\text{B}_{40}$ flux in the molar ratio 9:21:0.7 were put in an alumina crucible which was then sealed in a tantalum crucible. The sealed tantalum crucible was heated up to 1500°C under an argon atmosphere for a few hours and then cooled down slowly to 1100°C at a rate of 3°C h^{-1} and then to room temperature within 5 h. Crystals of YbNiB_4 were separated from the Ni–B flux by mechanical means. The structure of the sample was checked by using

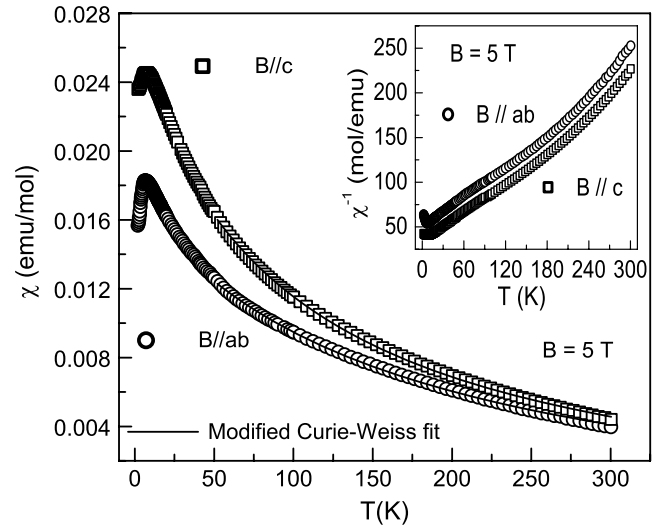


Figure 2. Magnetic susceptibility of YbNiB_4 as a function of temperature at a field of $B = 5$ T for both directions. The solid line is the fit to a modified Curie–Weiss relation. The inset shows the $\chi^{-1}(T)$ plot for $B \parallel ab$ and $B \parallel c$.

powder x-ray diffraction of crushed single crystals. For comparison purposes, a polycrystalline sample of the non-magnetic homologue LuNiB_4 was prepared by a standard arc melting procedure. Magnetization measurements on YbNiB_4 crystal were performed at various fields using a commercial superconducting quantum interference device magnetometer. Electrical resistivity and specific heat measurements were carried out using the AC transport and heat capacity options of a commercial physical properties measurement system (PPMS; Quantum Design).

3. Results and discussion

The powder x-ray diffraction pattern of crushed single crystal could be completely indexed with the YCrB_4 -type structure (space group $Pbam$) with lattice parameters $a = 5.8647 \text{ \AA}$, $b = 11.371 \text{ \AA}$ and $c = 3.3877 \text{ \AA}$. Our lattice parameters are in fair agreement with the reported ones $a = 5.8645 \text{ \AA}$, $b = 11.3680 \text{ \AA}$, $c = 3.3850 \text{ \AA}$ [22, 23]. Microprobe analysis of the surface of the platelet-like single crystals indicated a Yb:Ni ratio close to 1, but the B content could not be determined.

The magnetic susceptibility of YbNiB_4 in the temperature range 2–300 K for $B \parallel ab$ and $B \parallel c$ is shown in figure 2. The susceptibility is only weakly anisotropic, with χ_{ab} in the basal plane being smaller than χ_c along the c -axis. We did not observe an anisotropy within the basal plane. Susceptibility measurements with the field along two directions within the basal plane making an angle of 45° gave identical results. For all field directions, the susceptibility increases strongly below 300 K down to 8 K, suggesting a trivalent Yb state. The data plotted as $1/\chi(T)$ versus T follow a Curie–Weiss behavior, with an upward deviation at high temperatures probably associated with a diamagnetic contribution and a downward deviation below 100 K, as usually observed in trivalent Yb systems because of crystal electric field (CEF)

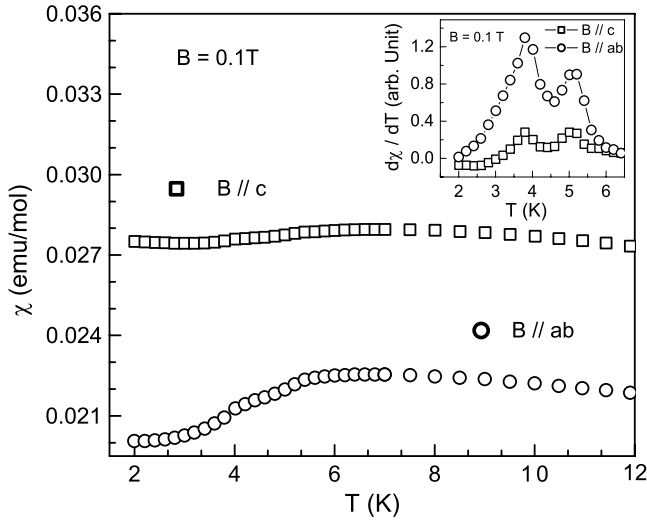


Figure 3. Low temperature magnetic susceptibility as a function of temperature for YbNiB₄ at $B = 0.1$ T for both directions. The inset shows the derivative of χ for $B \parallel ab$ and $B \parallel c$ at $B = 0.1$ T.

effects. A modified Curie–Weiss fit $\chi = \chi_0 + C/(T - \theta_p)$ above 100 K, with χ_0 accounting for diamagnetic and Van Vleck contributions, results in effective moments (per Yb) and Weiss temperatures of $\mu_{\text{eff}} = 5.06 \mu_B$ and $\theta_p = -159$ K for $B \parallel ab$, $\mu_{\text{eff}} = 4.64 \mu_B$ and $\theta_p = -96$ K for $B \parallel c$, as well as $\mu_{\text{eff}} = 4.73 \mu_B$ and $\theta_p = -124$ K for the powder average $\chi_{\text{av}} = (2\chi_{ab}(T) + \chi_c(T))/3$. The large value of the effective moment, being slightly larger than the value expected for a free Yb ion ($4.54 \mu_B$), confirms a trivalent Yb state. This difference might be due to crystal field effects or to a slight contribution of Ni. Below 20 K, the increase of $\chi(T)$ with decreasing T becomes weaker, and around 8 K $\chi(T)$ presents a broad maximum (see figure 3). Finally, two anomalies at $T_{N1} = 5.2$ K and $T_{N2} = 3.8$ K, associated with a decrease of $\chi(T)$, indicate the transition to an antiferromagnetic ordered state and a change in the antiferromagnetic structure, respectively. The anomalies are more pronounced for a field within the hard plane than for a field along the easy direction. These anomalies shift very slightly to lower temperatures with increasing field (see also discussion of the specific heat results). Magnetizations $M(B)$ at 2 K show a perfect linear increase of M with B . At this temperature the magnetization reaches only $0.205 \mu_B/\text{Yb}$ and $0.135 \mu_B/\text{Yb}$ for $B = 5$ T along the c direction and within the ab plane, respectively. Such a small value of magnetization at 5 T along the easy direction implies a rather strong antiferromagnetic exchange or/and a strong Kondo interaction. Extrapolating $M(B)$ for $B \parallel c$ linearly to higher field would lead to a saturation field of 50 T to reach the saturation moment $M_{\text{saturation}} = 2 \mu_B/\text{Yb}$ expected for a typical Yb CEF doublet! The presence of a large characteristic energy scale is supported by the weak field dependence of the transitions at T_{N1} and T_{N2} .

Thus our susceptibility results indicate a trivalent Yb state, ordering antiferromagnetically below $T_{N1} = 5.2$ K and showing a further AF transition at $T_{N2} = 3.8$ K. The large values of the Weiss temperature, the small values of the magnetization reached at 5 T, the weak field dependence

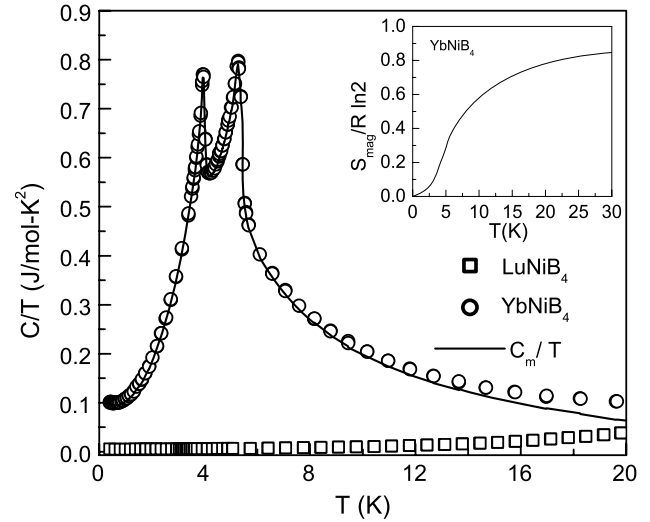


Figure 4. Specific heat of YbNiB₄, LuNiB₄ and the magnetic part as a function of temperature. Prominent anomalies due to magnetic transitions are clearly seen. The inset shows the T dependence of the magnetic entropy $S_{\text{mag}}(T)$.

of T_{N1} and T_{N2} all indicate a large energy scale of the indirect exchange or of the Kondo interaction. The presence of a maximum in $\chi(T)$ at a temperature larger than the antiferromagnetic ordering temperature is unusual. Such a maximum is either an indication of strong Kondo interactions or for low-dimensional and/or frustrated magnetic exchange. This will be discussed in more detail later.

In figure 4 we show in a plot of C/T as function of T the total specific heat of YbNiB₄ and LuNiB₄ as well as the magnetic part C_m/T obtained from the difference. We observe a continuous increase of C_m/T below 20 K ending in a lambda type anomaly at $T_{N1} = 5.3$ K, followed by a second lambda type anomaly of the same size at $T_{N2} = 4.0$ K. The large size of these anomalies confirms that both transitions are intrinsic to YbNiB₄. Below T_{N2} , C_m/T decreases strongly and merges below 1 K into a constant value corresponding to an enhanced Sommerfeld coefficient $\gamma = 100 \text{ mJ mol}^{-1} \text{ K}^{-2}$. We further plot in the inset of figure 4 the 4f related entropy $S_{\text{mag}}(T)$ obtained by integrating $C_m(T)/T$. $S_{\text{mag}}(T)$ reaches a value of $0.8R \ln 2$ at around 20 K where it starts to saturate, indicating that the first excited crystal electrical field doublet is well separated from the ground state doublet. Thus, only the latter one is relevant at low temperatures. The extended tail in C/T above T_{N1} is remarkable, and indicates strong fluctuations far above the long range ordering temperature. This is reflected in (i) a maximum value $C_{\text{max}} = 4.2 \text{ J mol}^{-1} \text{ K}^{-1}$ at T_{N1} well below the value $C_{\text{MF}} = 12.5 \text{ J mol}^{-1} \text{ K}^{-1}$ expected for a mean field transition in a doublet system, (ii) a reduced value of the entropy collected until T_{N1} , $S_{\text{mag}}(T_{N1}) = 0.32R \ln 2$ and (iii) the ordering temperature $T_{N2} = 5.3$ K being well below the characteristic energy scale of the 4f electrons $T_{4f} = 16$ K. Here we took as a direct and model independent estimate for T_{4f} twice the temperature where $S_{\text{mag}}(T)$ reaches $0.5R \ln 2$. Both for the case of the single ion Kondo effect [24] and of the Heisenberg spin chain [25], for which the specific heat has been calculated with a high precision, the relation $S(T = T_K/2$

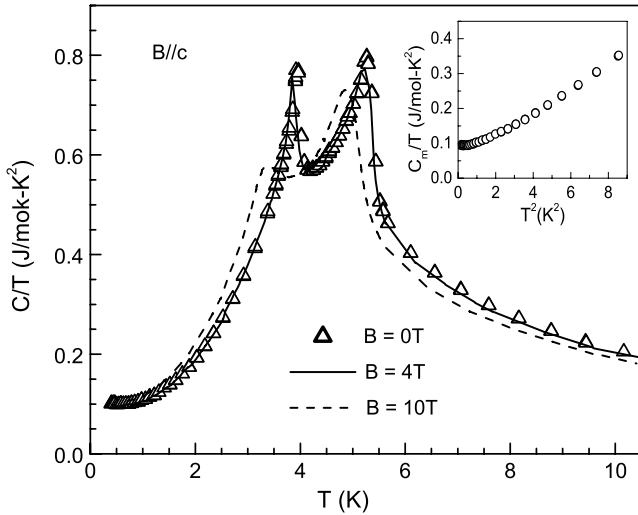


Figure 5. Field dependent specific heat of a YbNiB₄ single crystal for $B \parallel c$. The inset shows a C_m/T versus T^2 plot.

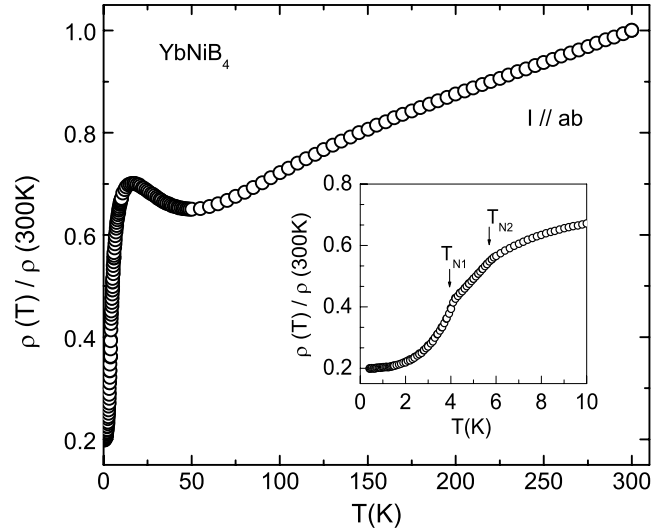


Figure 6. Zero field in-plane resistivity of YbNiB₄. The inset shows the low temperature resistivity.

or $T = J/2k_B = 0.5R \ln 2$ is fulfilled within 10%. Such strong fluctuations above T_N can again be attributed to two different mechanisms, either a strong Kondo interaction or low-dimensional and/or frustrated exchange. Application of a magnetic field along the easy c direction leads to only a slight shift of T_{N1} to lower temperatures, $T_{N1}(10 \text{ T}) = 4.8 \text{ K}$, while the anomaly at T_{N2} gets partially suppressed and shifts more strongly, $T_{N2}(10 \text{ T}) = 3.0 \text{ K}$ (see figure 5). We add in the inset of figure 5 a plot of C_m/T versus T^2 at low temperatures, which demonstrates that $C(T)$ decreases more strongly with T than T^3 , suggesting the presence of a small energy gap in the magnetic excitations, being a likely consequence of the weak Ising type anisotropy of this system.

Further insight can be obtained from the resistivity data, since Kondo type interactions lead to a large and strongly temperature dependent scattering of the conduction electrons by Yb 4f moments, while the effect of indirect exchange between these moments is much weaker. The temperature dependence of the normalized resistivity measured for current in the basal plane is shown in figure 6. While at high temperatures $\rho(T)$ of YbNiB₄ presents a standard metallic behavior with a linear decrease with T , below 45 K it increases again and show a broad maximum around 16 K. The decrease below 16 K is at first quite smooth, becoming more pronounced below T_{N1} and abrupt below T_{N2} (see inset of figure 6). This rapid decrease in resistivity below the transition temperature is due to the loss in spin disorder scattering. Below 2 K $\rho(T)$ merges into a constant residual resistivity leading to a residual resistivity ratio $\text{RRR} = \rho(300 \text{ K})/\rho(2 \text{ K}) = 4.5$, indicating a reasonably good quality for our single crystals. The absolute value of resistivity at room temperature is around $\approx 250 \mu\Omega \text{ cm}$. We have also measured the magnetoresistance at $T = 2$ and at 50 K for $B \parallel c$ and $I \parallel ab$ (see figure 7). In the ordered state at 2 K the magnetoresistance is positive, nicely follows a B^2 power law and reaches a value of 16% at 7 T. A positive magnetoresistance proportional to B^2 is expected for a Fermi liquid at low temperatures.

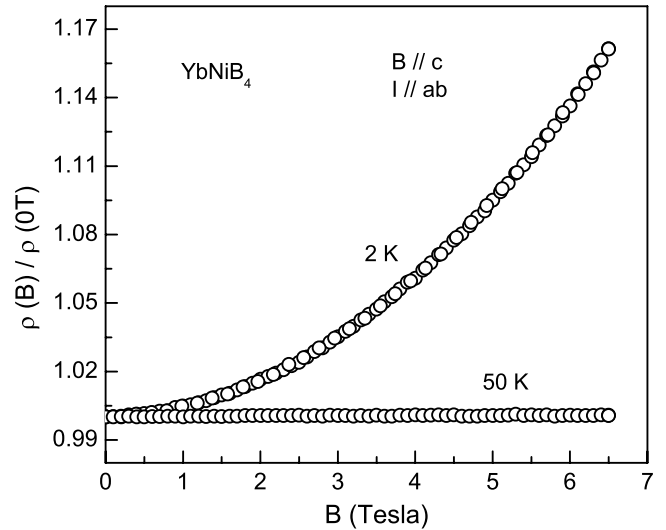


Figure 7. Magnetoresistance at 2 and 50 K as a function of magnetic field for $I \parallel ab$ and $B \parallel c$.

The increase of $\rho(T)$ between 50 and 16 K, as well as the broad maximum at a temperature far above T_{N1} provide evidence for the presence of a Kondo interaction. However, at T_{N1} , $\rho(T)$ still amounts to 80% of its value at the maximum, while in typical Kondo lattices with $T_N \ll T_K$, like for example CeCu₂Si₂, most of the spin disorder scattering has already disappeared at T_N because the coherent Kondo state is already quite well established at $T_N \ll T_K$. In contrast, one can also attribute the decrease of $\rho(T)$ between 16 K and T_{N1} observed in YbNiB₄ to the onset of antiferromagnetic correlations, in accordance with the maximum in $\chi(T)$ and the extended high temperature tail in $C(T)$. Therefore the resistivity data indicate the presence of Kondo interaction, but suggest that it is not the only origin of the large fluctuations above T_N . This is also supported by the Sommerfeld coefficient $\gamma = 100 \text{ mJ mol}^{-1} \text{ K}^{-2}$, which is enhanced, but not as much as one would expect for a system with $T_N = 1/3T_K$.

The strongest evidence for the relevance of low-dimensional antiferromagnetic fluctuations is given by the broad but well defined maximum in $\chi(T)$ above T_N . In oxide or organic spin systems such maxima are hallmarks for low-dimensional antiferromagnetic fluctuations. The structure of YbNiB_4 provides arguments both for dominant one-dimensional exchange or dominant two-dimensional exchange. On the one hand it presents a clear layered structure, favorable for 2D interactions. On the other hand the distance between nearest Yb neighbors along the c direction is very short, $d_{\text{Yb-Yb}} = c = 3.3877 \text{ \AA}$, less than twice the atomic radius of trivalent Yb ($\approx 3.44 \text{ \AA}$). This could lead to a dominant magnetic exchange along the c direction.

4. Conclusion

To summarize, we have grown YbNiB_4 single crystals using a Ni-B flux and determined the magnetic properties of this compound by means of magnetization, specific heat and resistivity measurement. In YbNiB_4 the Yb ions are in a trivalent state and order antiferromagnetically at $T_{N1} = 5.3 \text{ K}$. A second transition to a different AF state occurs at $T_{N2} = 4.0 \text{ K}$. The susceptibility is weakly anisotropic, χ along the c -axis being slightly larger than within the basal plane of the orthorhombic YCrB_4 -type structure. Large values of the Weiss temperatures for both field directions, small values of the magnetization at 5 T at low temperatures and a rather weak field dependence of T_{N1} and T_{N2} all indicate a large energy scale for the magnetic interactions, which was estimated to be $T_{4f} = 16 \text{ K}$ from an analysis of the T dependence of the entropy. On the other hand the extended tail observed in C_m/T above T_N , the small value of the peak specific heat at T_{N1} , the reduced value of the entropy collected until T_{N1} and the large T_{4f}/T_N ratio indicate strong fluctuations in an extended temperature range above T_N . An increase in $\rho(T)$ between 50 and 16 K leading to a broad maximum at a temperature far above T_{N1} , as well as an enhanced Sommerfeld coefficient $\gamma = 100 \text{ mJ mol}^{-1} \text{ K}^{-2}$, provide evidence that part of these fluctuations are due to a significant Kondo interaction. But since the Kondo behavior in $\rho(T)$ is much less pronounced than expected for a Kondo lattice with $T_K = 16 \text{ K}$, we suspect an additional mechanism leading to strong fluctuations. The broad but well defined maximum in $\chi(T)$ above T_{N2} for both field directions as well as the features of the YCrB_4 -type structure, which provides arguments for strong one-dimensional or strong two-dimensional exchange, suggest low-dimensional fluctuation to be relevant in this system. However the question about the respective importance of Kondo versus low-dimensional fluctuations, as well as the direction of the strongest exchange path, cannot be solved with the present results and deserves further investigations.

Acknowledgment

Financial assistance from BRNS (grant no. 2007/37/28/BRNS) is acknowledged.

References

- [1] Trovarelli O, Geibel C, Mederle S, Langhammer C, Grosche F M, Gegenwart P, Lang M, Sparn G and Steglich F 2000 *Phys. Rev. Lett.* **85** 626
- [2] Gegenwart P, Custers J, Geibel C, Neumaier K, Tayama T, Tenya K, Trovarelli O and Steglich F 2002 *Phys. Rev. Lett.* **89** 056402
- [3] Hossain Z, Geibel C, Weickert F, Radu T, Tokiwa Y, Jeevan H, Gegenwart P and Steglich F 2005 *Phys. Rev. B* **72** 094411
- [4] Yuan H Q, Nicklas M, Hossain Z, Geibel C and Steglich F 2006 *Phys. Rev. B* **74** 212403
- [5] Torikachvili M S, Jia S, Mun E D, Hannahs S T, Black R C, Neils W K, Martien D, Budk'o S L and Canfield P C 1997 *Proc. Natl Acad. Sci. USA* **104** 9960
- [6] Muramatsu T, Kanemasa T, Bauer E, Giivannini M, Kagayama T and Shimizu K 2007 arXiv:0704.3307v1
- [7] Jeevan H S, Geibel C and Hossain Z 2006 *Phys. Rev. B* **73** 02047
- [8] Kim M S, Bennett M C and Aronson M C 2008 *Phys. Rev. B* **77** 144425
- [9] Ku H C and Yu H 1986 *Phys. Rev. B* **34** 1974
- [10] Fertig W A, Johnston D C, DeLong L E, McCallum R W, Maple M B and Matthias B T 1977 *Phys. Rev. Lett.* **38** 987
- [11] Matthias B T, Corenzwit E, Vandenberg J M and Barz H E 1997 *Proc. Natl Acad. Sci. USA* **74** 1334
- [12] Kasuya T 1994 *Europhys. Lett.* **26** 277
- [13] Kim J Y, Cho B K, Lee H J and Kim H C 2007 *J. Appl. Phys.* **101** 09D501
- [14] Yatskar A, Budraa N K, Beyermann W P, Canfield P C and Bud'ko S L 1996 *Phys. Rev. B* **54** 3772
- [15] Boothroyd A T, Barratt J P, Bonville P, Canfield P C, Murani A, Wildes A R and Bewley R I 2003 *Phys. Rev. B* **67** 104407
- [16] Sobczak R and Rogl P 1979 *J. Solid State Chem.* **27** 343
- [17] Ku H C and Lin D C 1987 *J. Less-Common Met.* **127** 35
- [18] Okada S, Shishido T, Mori T, Kudou K, Iizumi K, Lundström T and Nakajima K 2006 *J. Alloys Compounds* **408** 547
- [19] Macaluso R T, Nakatsuji S, Kuga K, Thomas E L, Machida Y, Maeno Y, Fisk Z and Chan J Y 2007 *Chem. Mater.* **19** 1918
- [20] Nakatsuji S, Kuga K, Machida Y, Tayama T, Sakakibara T, Karaki Y, Ishimoto H, Yonezawa S, Maeno Y, Pearson E, Lonzarich G G, Balicas L, Lee H and Fisk Z 2008 *Nat. Phys.* **4** 603
- [21] Nagamatsu J, Nakagawa N, Muranaka T, Zenitani Y and Akimitsu J 2001 *Nature* **410** 63
- [22] Veremchuk I, Prots Y, Leithe-Jasper A and Kuz'ma Y 2005 *Z. Kristallogr. NCS* **220** 125
- [23] Veremchuk I, Chaban N and Kuzma Y B 2006 *J. Alloys Compounds* **413** 127
- [24] Desgranges H U and Schotte K D 1982 *Phys. Lett. A* **91** 240
- [25] Klümper A and Johnston D C 2000 *Phys. Rev. Lett.* **84** 4701